Eur Spine J (2007) 16:2215–2224
DOI 10.1007/s00586-007-0501-0

ORIGINAL ARTICLE

Effect of Hydroxyapatite porous characteristics on healing outcomes in rabbit posterolateral spinal fusion model

Makoto Motomiya · Manabu Ito · Masahiko Takahata · Ken Kadoya · Kazuharu Irie · Kuniyoshi Abumi · Akio Minami

Received: 7 February 2007 / Revised: 30 June 2007 / Accepted: 3 September 2007 / Published online: 22 September 2007

Abstract Hydroxyapatite (HA) has been commonly used as a bone graft substitute in various kinds of clinical fields. To improve the healing capability of HA, many studies have been performed to reveal its optimal structural characteristics for better healing outcomes. In spinal reconstruction surgery, non-interconnected porous HAs have already been applied as a bone graft extender in order to avoid autogenous bone harvesting. However, there have been few experimental studies regarding the effects of the structural characteristics of HA in posterolateral lumbar intertransverse process spine fusion (PLF). The aims of this study were to investigate the effect of HA porous characteristics on healing outcomes in a rabbit PLF model in order to elucidate appropriate structural characteristics of HA as a bone graft extender. Thirty-six adult female Japanese White rabbits underwent bilateral intertransverse process fusion at the level of L5–6 without internal fixation. We prepared three types of HA with different porosities: HA with 15% porosity (HA15%), HA with 50% porosity (HA50%), and HA with 85% porosity (HA85%), all of which were clinically available materials. The HA15% and HA50% had few interconnecting pores, whereas the HA85%, which was a recently developed material, had abundant interconnecting pores. All rabbits were randomly divided into the following four groups according to the grafted materials: (1) HA15% + autogenous bone, (2) HA50% + autogenous bone, (3) HA85% + autogenous bone, (4) pure autogenous bone graft. The animals were euthanized at 5 weeks after surgery, and post-mortem analyses including biomechanical testing, radiographical and histological evaluations were performed. There was no statistically significant difference in either fusion rate and/or bending stiffness among the three HA groups. However, in histological and radiological analyses, both bone ingrowth rate and direct bone bonding rate in the HA85% group were significantly higher than those in the HA15% and HA50% groups, despite the similar value of bone volume rate in fusion mass among the three HA groups. In the HA85% group, bone ingrowth was achieved throughout the implanted HAs via interconnecting pores and there was excellent unification between the HA granules and the newly mineralized bone. On the other hand, in the non-interconnected porous HA groups, only a little bone ingrowth could be seen at the peripheral pores of the implanted HA, and its surface was mostly covered with fibrous tissue or empty space. The current study demonstrated that the HA porous characteristics had an effect on the histological outcomes in a rabbit PLF model. We would like to conclude that the interconnected high porous structure seems to be promising for the environment of PLF in the point of producing fusion mass with higher cellular viability. This is because the HA85% is superior in terms of integration with the newly formed bone in fusion mass compared to the non-interconnected porous HAs. However, the porous modifications of HA have little influence on fusion rate and mechanical strength because primary stabilization of the fusion segment is mainly achieved by bridging bone between the adjacent transverse processes outside the implanted materials, rather than the

M. Motomiya · M. Ito (✉) · M. Takahata · K. Kadoya · K. Abumi · A. Minami
Department of Orthopaedic Surgery,
Hokkaido University Graduate School of Medicine,
Kita-15 Nishi-7, Kita-ku, Sapporo 060-8638, Japan
e-mail: maito@med.hokudai.ac.jp

K. Irie
Department of Oral Anatomy, Health Sciences
University of Hokkaido School of Dentistry,
Ishikari-Tobetsu, Japan

degree of integration between the newly formed bone and the HA granules in PLF.

Keywords Bone graft substitute · Hydroxyapatite · Spine fusion · Porous characteristics · Interconnecting pore

Introduction

Bone graft surgeries have been widely performed in various fields such as orthopaedic, craniomaxillofacial, dental, and plastic surgery. Autogenous bone has been commonly used for bone graft surgery as the gold standard material. However, there have been a lot of morbidities associated with the harvest of autogenous bone such as long-lasting pain, deep infection, vascular injuries, and blood loss at the donor site [28, 33]. The limited volume of autogenous bone is also a disadvantage, especially in the case of patients with osteoporosis or with multiple previous bone graft procedures [3, 4, 27]. Therefore many researchers have developed and studied various kinds of bone graft substitutes in order to avoid bone graft harvesting.

Of all bone graft substitutes, Hydroxyapatite (HA) is one of the most popular materials and has been utilized experimentally and clinically in bone graft surgery because HA is a biocompatible material with excellent osteoconductivity [10, 20, 21]. However, clinical outcomes of the conventional HAs have not been superior to that of autogenous bone graft. In order to improve the healing capability of HA in bone graft surgery, many studies have been performed to reveal its optimal structural characteristics for bone healing [8, 9, 18, 19]. For example, for the non-weight bearing applications such as metaphyseal bone defects, the optimal porous structure of HA is believed to be the interconnected high porous structure with suitable pore size of approximately 300 μm [8, 9]. Tamai et al. [29] reported that abundant interconnected space promotes infiltration of bone tissue, bone marrow, and blood vessels, and allows bone remodeling throughout the material. On the other hand, for the weight-bearing applications such as spinal interbody fusion, a dense HA with adequate mechanical strength is beneficial to support the operated segment [16, 32]. Although high porous structure of HA is also preferable for spinal interbody fusion in terms of its superior integration with host bone tissue, this structure of HA cannot withstand severe cyclic mechanical loading. In this way, it is important to choose the proper structural characteristics of HA according to grafted environments.

Posterolateral lumbar intertransverse process spine fusion (PLF) is a commonly performed bone graft surgeries [4]. In PLF, the conventional non-interconnected porous HA has already been applied as bone graft extenders [4, 27, 30]. However, most surgeons are using it without consideration of the effects of its porous characteristics on healing outcomes in PLF. As many researchers reported, the grafted environment of PLF is significantly different from those of other operations such as metaphyseal bone defect and spinal interbody fusion in the following two points [4, 5, 27]. The first is that grafted materials in the environment of PLF are exposed to excessive distraction or tension loads, which may cause non-union of the fusion segment. Second is that the grafted materials are surrounded by less osteogenic environments such as muscle and other soft tissues, not bone tissue. Despite the above-mentioned unique environment of the grafted site, to our knowledge there has been little information about optimal porosity and geometrical porous design of HA as a bone graft extender in PLF.

The purpose of this study was to investigate the effect of HA porous characteristics on healing outcomes in a rabbit PLF model in order to elucidate appropriate structural characteristics of HA as a bone graft extender.

Materials and methods

Material preparation

We prepared three types of HA with different porosities (15, 50, and 85%) for this PLF experiment. The HAs with 15% porosity (HA15%) and with 50% porosity (HA50%) (APACERAM, PENTAX Corp., Tokyo, Japan) are conventionally available materials. Whereas the HA with 85% porosity (HA85%) (APACERAM-AX, PENTAX Corp., Tokyo, Japan), the highest among the clinically available HAs, has recently been developed using a new technique [26].

The structural characteristics of each HA under a scanning electron microscope (SEM) are shown in Fig. 1. As shown in Fig. 1a, d, the HA15% had a mostly dense body with scattered small-sized macropores. Figure 1b, e showed that the HA50% had many solitary large-sized macropores. There were few porous interconnections between each macropore in the HA15% and HA50%. On the other hand, SEM photographs of the HA85% showed that the material had a cancellous bone-like structure with abundant interconnecting pores and a microporous surface in every macropore (Fig. 1c, f). The detailed porous characteristics of each HA are listed in Table 1. As shown in Table 1, initial compressive strength gradually decreases in correlation with increasing porosity.

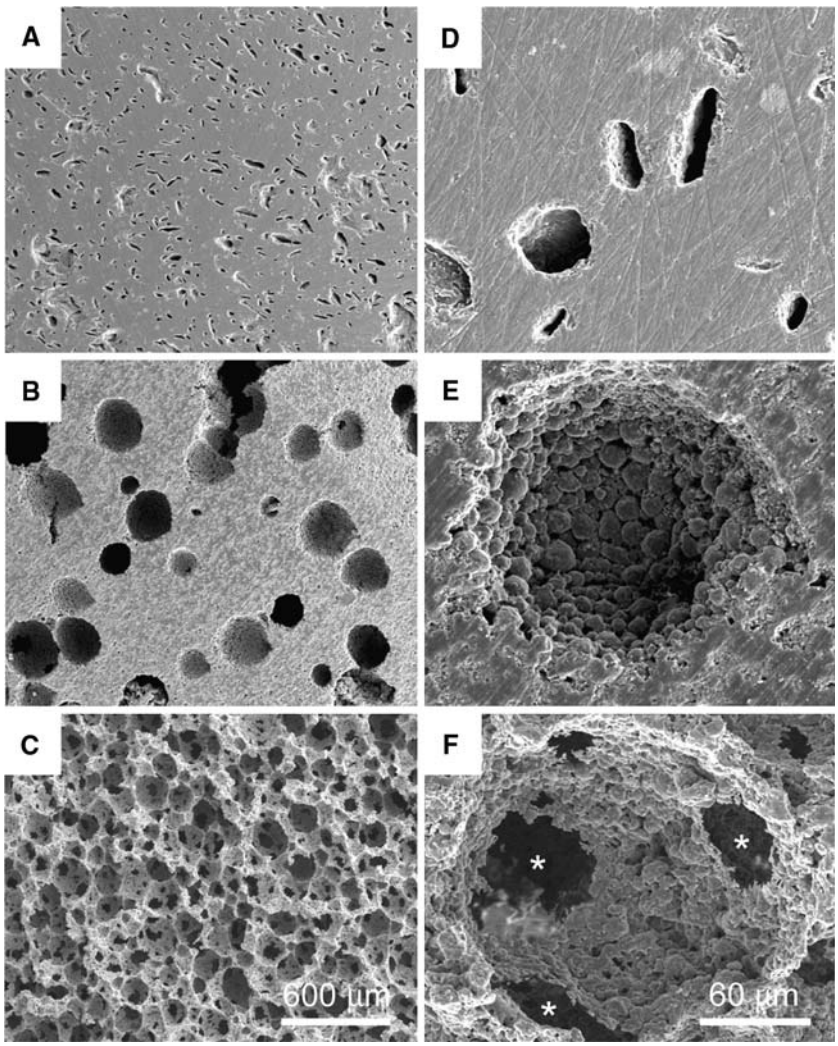

Fig. 1 Scanning electron microscopic appearance of the HA surface. **a**, **d** The HA15% has a mostly dense body with scattered small-sized macropores. **b**, **e** The HA50% has many solitary large-sized macropores. Each macropore has microporous surface and few porous interconnections. **c**, **f** The HA85% has a cancellous bone-like structure with abundant interconnecting pores (*asterisk*) about 50 μm in diameter and a microporous surface in every macropore

Table 1 The porous characteristics of HA

	Porosity (%)	Interconnecting pores	Pore size (μm)	Initial strength (MPa)
HA15%	15	–	10–50	240
HA50%	50	–	50–500	30
HA85%	85	+ (Average 90 μm)	50–300	2

Experimental posterolateral spine fusion in a rabbit model

The experimental protocol of this animal study was reviewed and approved by the Institutional Animal Care and Use Committee. Thirty-six adult female Japanese White rabbits (2.9–3.4 kg) were obtained from CLEA Japan, Inc. and were divided into the following four groups according to the grafted materials:

(1) HA15% + autogenous bone (n = 11)
(2) HA50% + autogenous bone (n = 9)
(3) HA85% + autogenous bone (n = 10)
(4) Pure autogenous bone graft (Auto) (n = 6)

Operative procedure

All rabbits underwent bilateral intertransverse process arthrodesis at the level of L5–6 without internal fixation [7]. General anesthesia was induced with an intravenous administration of sodium pentobarbital (20 mg/kg) and maintained with 2% isoflurane. Just before surgery Benzylpenicillin Potassium (Penicillin G Potassium, Meiji Seika, Tokyo, Japan; 5,000 U/kg) was injected into the quadriceps muscle for antibiosis. The rabbits were placed prone on the surgical table and shaved. A dorsal midline skin incision was made and the bilateral transverse processes of L5 and L6 were exposed through the intermuscular plane between the multifidus and longissimus muscles [31]. The transverse processes were

decorticated using an electric burr. Autogenous cortico-cancellous bone was harvested from the iliac crest through extended fascial incisions. In the HA groups, 1.5 ml of cubic shaped HA granules (3–4 mm in width) and an equal amount of morselized autogenous iliac bone were mixed and grafted to the intertransverse space at L5–6 bilaterally. In the Auto group, 3.0 ml of pure autogenous iliac bone was grafted. After irrigation, the fascial incisions were closed with 3-0 absorbable sutures and the skin was closed with 3-0 nylon sutures.

All rabbits were housed one per cage and allowed an ad libitum diet and water. Their neurological conditions and general health were checked each day. At postoperative five weeks, all animals were euthanized with an intravenous administration of sodium pentobarbital (200 mg/kg bolus) and the lumbar spinal segment from L1 to S2 was removed en bloc with the surrounding soft tissue. An operative segment was carefully retrieved and postmortem analyses including biomechanical testing, radiographical and histological evaluations were performed.

Manual palpation and biomechanical testing

The operative segments were gently trimmed off all the soft tissue. Fusion status was assessed according to the magnitude of the flexion-extension motion of the segments by manual palpation [7]. They were graded as fused or not fused by two independent orthopaedists who were blinded to the experimental group of the animal.

All spines were stored in sealed double-plastic bags at –28°C until preparation for testing. Before biomechanical testing, each specimen was completely thawed at room temperature. Each fusion mass was evaluated by non-destructive three-point bending testing using the biomechanical testing machine (858 Mini Bionix II, MTS System Co., Minneapolis, MN, USA) [11]. The schema of biomechanical testing is shown in Fig. 2a. A small jig was designed to hold the motion segment and to allow three-point bending tests at the center of the fused disc space. The adjacent vertebral bodies were placed with their dorsal sides down on two fulcra separated by 25 mm. The upper anvil (7.0 mm in diameter) was placed to apply a load on the ventral surface of the intervertebral disc vertical to the longitudinal spine. A preload of 10 N was applied to the specimen, and the crosshead was zeroed at this point. The specimen was then cyclically preconditioned with 5 cycles to 0.5 mm of deformation at a rate of 0.4 mm/s. A load was applied to 2.0 mm of the deformation at a rate of 0.1 mm/s. The stiffness of the motion segment was defined as the linear slope of the load-displacement curve at 1.5 mm of deformation. Two load-displacement curves were obtained in each specimen, and the average stiffness was used as the representative value. The stiffness of the unsuccessful fusion segments defined by the manual palpation could not be calculated by the three-point bending testing because those segments showed more than 1 mm of deformation under the 10 N of the preload, and therefore the unsuccessful fusion segments were excluded from the three-point bending testing.

Radiographical and histological evaluations

Following mechanical tests, the specimens in each group were subjected to undecalcified tissue processing. The specimens were fixed in 70% ethanol for about 1 week. After fixation, they were dehydrated sequentially in 70, 80, 90 and 100% ethanol and were embedded in polyester resin. Two sections from each specimen were cut with a crystal microtome at a thickness of 500 μm. The cutting lines were parallel to the spinal longitudinal axis at 5 mm from the lateral edge of the intervertebral disc. The schema of cutting lines is shown in Fig. 2b. The sections were

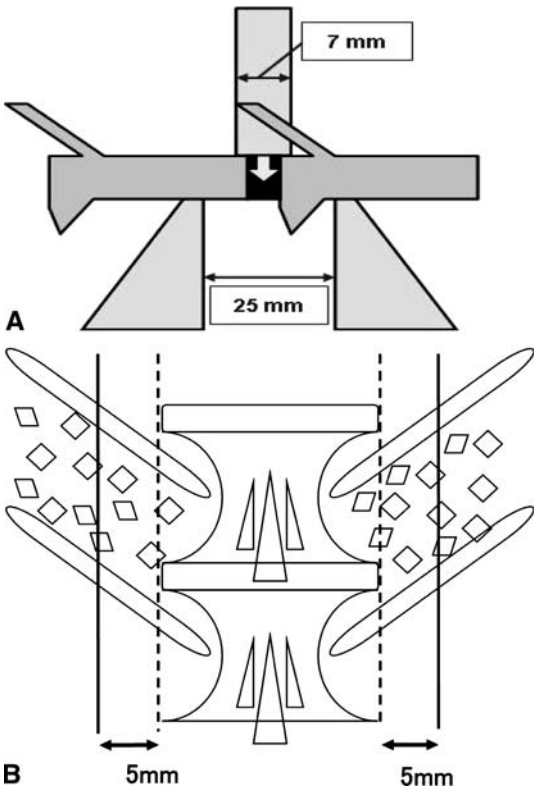

Fig. 2 **a** The schema of the three-point bending test of the operative segment. **b** The schema of the cutting lines for histological section. *Solid lines* indicate cutting lines, and *broken ones* indicate the lateral edges of the intervertebral disc

polished to a thickness of 500–80 μm and observed by contact microradiography (CMR) and light microscopy.

Contact microradiography

The section was mounted on a high-resolution film (SO-181; Kodak Co., Tokyo, Japan) and CMR was taken using a soft X-ray unit (SRO-M50D; Tanaka X-ray MFG. Co. Ltd, Tokyo, Japan) at 14.0 kVp, 2 mA, and an exposure time of 18 min. Newly formed mineralized bone within and around the implanted HA was investigated from the extent of radiographical density.

Histological analyses

After taking CMR, all sections were stained with Toluidine blue O and evaluated with a light microscope. For quantitative analysis, the images of those sections were captured through a light microscope. The mineralized bone area, which had been stained blue purple by Toluidine blue O staining, was then highlighted for measurement. The following parameters were calculated based on the dimensional data measured by "Win roof" software (Mitani Co., Fukui, Japan): bone ingrowth ratio (BIR), bone apposition ratio (BAR), BV/TV, and bone volume ratio outside implant (BV/TV_{out}). Bone ingrowth ratio was determined as the ratio of combined total bone volume within each HA to the combined total pore volume of HA [15]. Bone apposition ratio was the ratio of the combined total length of direct bone bonding to each HA to the combined total length of each HA in fusion mass [22]. BV/TV was measured as a ratio of bone volume within fusion mass, while BV/TV_{out} was measured as a ratio of bone volume within fusion mass outside the implanted granules. The values for each parameter were determined separately for the left and right side fusion mass in each rabbit. Each section was calculated two times by a single observer, and the two values were averaged.

Statistical methods

All parameters were analyzed by analysis of variance (ANOVA). Fusion rates among the groups were compared using Fisher's exact test. The biomechanical and histological evaluations among groups were calculated by ANOVA combined with a Fisher's-protected least-significant difference (Fisher's PLSD) or Bonferroni multiple comparison test when appropriate (StatView, SAS Institute Inc. Cary, NC, USA). The results were expressed as the mean ± standard deviation (SD), and were considered statistically significant at $P < 0.05$.

Results

All rabbits survived the surgery, and ambulated one day later. A total of six animals, including three from the HA15% group, one from the HA50% group, and two from the HA85% group, died from deep wound infections and were excluded from the study. Because of the high incidence of infection in the early series of the animals in this study, the draping and irrigation techniques at the surgical site were modified and the animals were treated with an additional short course of antibiotic therapy in the later series.

Manual palpation and biomechanical testing

The manual palpation test showed that the fusion rates in the three HA groups ranged from 60 to 75% in this PLF model, and there was no significant difference between each HA group. In the Auto group fusion rate was 100%, which was higher than those in the HA groups. However, the difference was not significant (Table 2).

The result of the three-point bending testing showed that the bending stiffness in the HA15% group was lower than those in the other three groups. However, there was no significant difference in the bending stiffness among the four groups (Table 2).

Contact microradiography

CMR photographs in the HA15% group showed that direct bonding between the surface of the HA and the newly mineralized bone was seen in a limited area (Fig. 3a). In the HA50% group, there was also only a little direct bone bonding with the implant and bone ingrowth could be seen only in peripheral pores of the HA granule (Fig. 3b). On the other hand, the newly mineralized bone formed deeply inside the HA85% granules and bonded directly with the implanted materials in the fusion mass. The newly formed bone inside the HA85% remained connected to the bone tissue outside the material (Fig. 3c). High magnification

Table 2 Fusion rate and bending stiffness of fusion mass

Group	Number (%) of fused specimen	Bending stiffness (N/mm)
HA15%	5/8 (62.5)	99.3 ± 52.0
HA50%	6/8 (75.0)	127 ± 2.0
HA85%	5/8 (62.5)	122 ± 47.5
Auto	6/6 (100)	123 ± 38.6

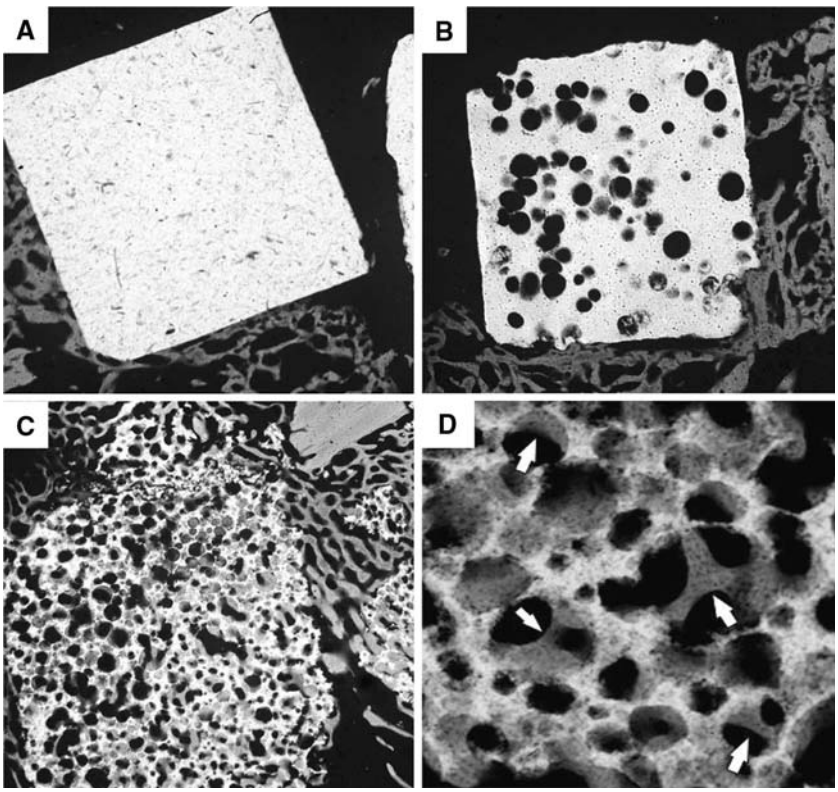

Fig. 3 Contact microradiographs of the sagittal section of the fusion mass containing the HA granules. In the HA15% group (**a**) and HA50% group (**b**), there is only a little direct bonding between the HA granules (*white*) and the newly mineralized bone (*gray*). On the other hand, in the HA85% group (**c**, **d**), there is excellent unification between the HA (*white*) and newly mineralized bone (*gray*). *Arrows* show newly mineralized bone within pores of the HA85% granule (magnification: **a**–**c** ×5, **d** ×30)

photographs showed an excellent unification between the HA and the newly trabecular bone (Fig. 3d).

Histological analyses

In histological findings of the Auto group, both bone and cartilage formation could be seen at the intertransverse space of L5–6. The grafted bone was integrated with the newly formed trabecular bone within the fusion mass at 5 weeks after implantation (Fig. 4a).

Distinct histological differences were observed among the HA groups. In the HA15% and HA50% groups, microphotographs showed that bone ingrowth could be seen only in peripheral pores of the HA granules and its surface was mainly covered with fibrous tissue or empty space (Fig. 4b, c, e, f). Although bridging bone was formed between the L5 and L6 transverse process in these specimens, there was only a little direct bone bonding with the HA granules. On the other hand, in the HA85% group, bone ingrowth was achieved throughout the HA granules via the interconnecting pores and the amount of direct bone bonding area was the largest among the three HA groups (Fig. 4d, g). The HA85% was integrated with the newly formed bone in the fusion mass. Middle magnification microphotographs in the HA85% group showed that the newly formed bone covered the microporous surface of macropores inside the material (Fig. 4h). High magnification microphotographs in the HA85% also showed the presence of osteoblast-like cells attached to the rough surface of macropores (Fig. 4i).

Quantitative histological evaluation showed that the average BIR was the highest in the HA85% group (24.0%), and lower in the HA15% (0%) and the HA50% groups (2.0%) (Fig. 5a). The average BAR in the HA85% group (14.3%) was also superior to those in the HA15% (4.8%) and the HA50% group (6.2%) with a statistical significance (Fig. 5b). The average BV/TV were 19.4, 22.4, 24.5, and 40.6% in the HA15%, HA50%, HA85%, and the Auto groups, respectively (Fig. 5c). The average BV/TV_{out} were 26.9, 31.9, and 30.8% in the HA15%, HA50%, and HA85% groups respectively (Fig. 5d). The Auto group showed the highest BV/TV among the four groups, which was statistically significant (Fig. 5c). While, there was no statistically significant difference among the three HA groups in the BV/TV_{out} (Fig. 5d).

Discussion

Owing to the progress in production methods of HA, HA can now be controlled in its porosity and even in the dimensions of the pores themselves through manufacturing processes. Many researchers have reported that porous modifications of HA achieved successful healing outcomes in various sites such as metaphyseal bone defects. However, there have been few studies related to the significance

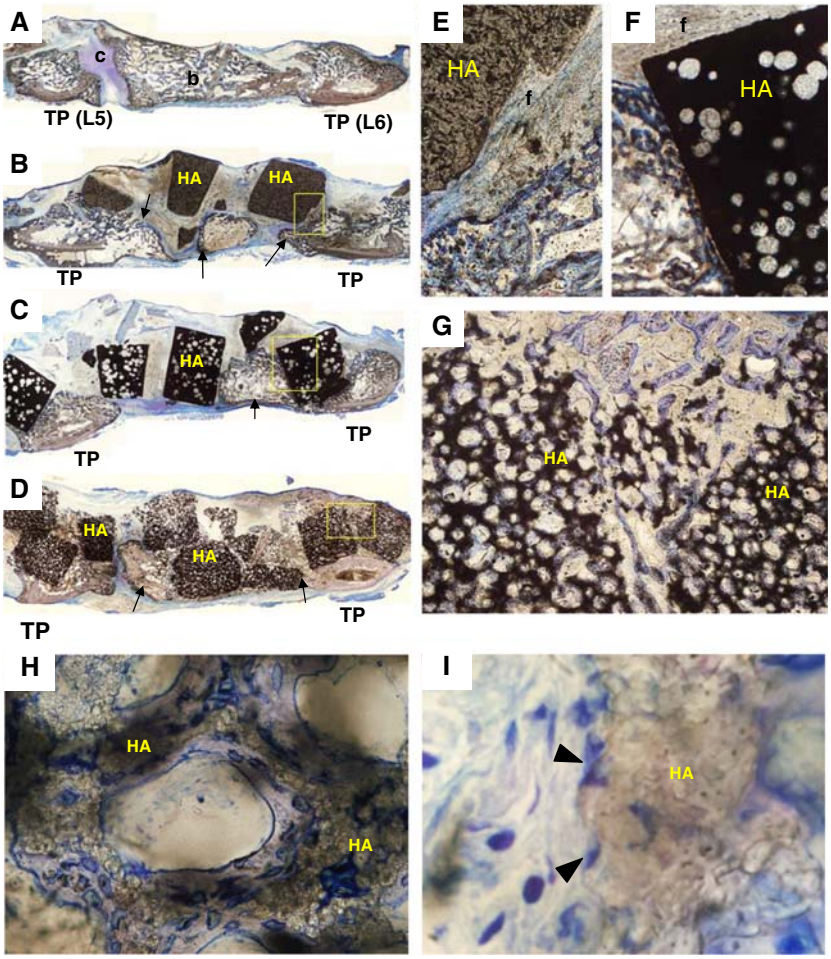

Fig. 4 Histological sagittal sections of the fusion mass stained with Toluidine Blue O in a rabbit PLF model (**a**–**i**). In the Auto (**a**) group, both bone (**b**) and cartilage (**c**) formation can be seen between the L5 and L6 transverse process (*TP*). In the HA15% (**b**, **e**) and the HA50% (**c**, **f**) group, newly formed bone (*arrows*) can be seen between the L5 and L6 transverse process. However, there is only a little direct bone bonding with the HA granules. In these specimens, most surfaces of the HA granules are surrounded by fibrous tissue (**f**), and bone ingrowth is obtained only in peripheral pores of the implanted HA. In the HA85% (**d**, **g**) group, newly formed bone integrates with the HA granules and bone ingrowth is achieved throughout the materials. High magnification photographs in the HA85% (**h**, **i**) group show newly formed bone (*blue–purple*) covers the microporous surface in each macropore of HA (*brown*) and many osteoblast-like cells (*arrowheads*) are seen attached to the rough surface of the HA (magnification: **a**–**d** ×1, **e**–**g** ×5, **h** ×50, **i** ×250)

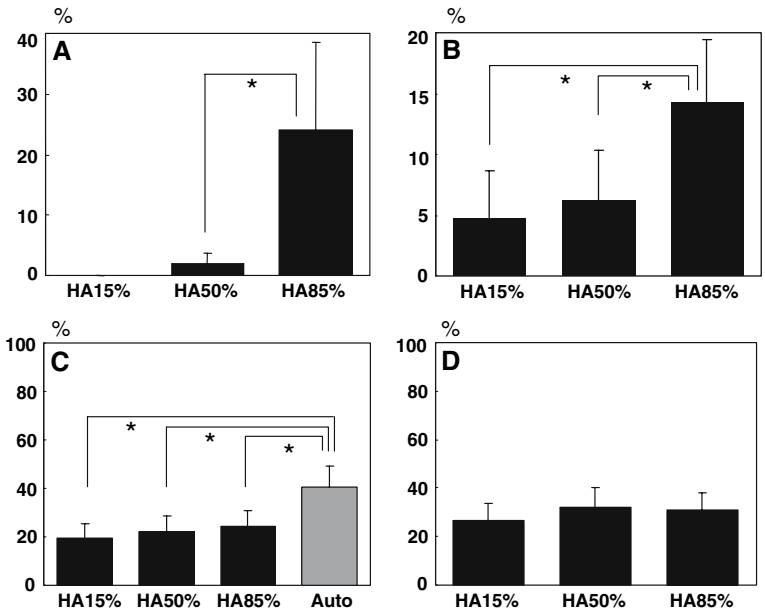

Fig. 5 The results of quantitative histological analysis of the fusion mass. The bone ingrowth rate (*BIR*) (**a**) and the bone apposition rate (*BAR*) (**b**) are higher in the HA85% group compared to those in the HA15% and HA50% group. In contrast, there is no significant difference among the three HA groups in the bone volume rate outside the implanted granules (BV/TV_{out}) (**d**), although it is significantly higher in the Auto group than any other groups in the bone volume rate (BV/TV) (**c**). (mean ± SD, * $P < 0.05$)

of HA porous structure in PLF. In the current study, we hypothesized that HA porous characteristics also had an influence on healing outcomes in PLF. We investigated this hypothesis using three types of HA with different porosities as a bone graft extender in a rabbit PLF model.

The histological results of this study showed the superiority of the HA85% in both osteoconduction and osteointegration compared to the HA15% and HA50% in a rabbit PLF model, although there was no significant difference in fusion rate and mechanical strength between the three HA groups. We believe that this superiority of the HA85% derives not only from the high porosity but also from the abundant interconnecting pores. This is because the interconnected porous structure has been reported to be the most important for osteoconduction and osteointegration among various porous parameters [1, 29]. Since cell migration, mineralization, and subsequent bone remodeling depend on vessel ingrowth, the vascularization through the interconnecting pores is indispensable for bone ingrowth and for maintaining cellular viability in the material. In the HA85% group there were abundant osteogenic cells and mineralized trabecular bone throughout the implanted granules at five weeks after implantation in this PLF model. We observed that the newly formed bone inside the materials remained connected to the bone tissue outside them via the interconnecting pores. In addition, few differences in the histological results between the HA15% and the HA50% indicate that the porous interconnection of HA is more important than its porosity in PLF. On the basis of these results, we reasonably conclude that the interconnecting pores of HA also have a significant influence on the healing outcomes in the environment of PLF.

Moreover, the microporous structure in every macropore possibly contributed to the excellent histological outcomes in the HA85% group, although its effect on the behavior of bone healing is still controversial. Some researchers reported that the micropores (<10 μm in diameter) would not be permissive to osteoconduction because the size of the nucleus in most mammalian cells is more than 10 μm [24, 29]. On the other hand, Annaz et al. [2] reported that the microporous surface played a role in initial cellular anchorage and attachment of osteogenic cells [14]. Habibovic et al. demonstrated that modification of the microporous surface affected the interface dynamics of the ceramic in such a way that relevant cells were triggered to differentiate into the osteogenic lineage [12, 13, 25, 34]. After 5 weeks implantation, many osteoblast-like cells were settled on the microporous surface of macropores within the HA85% granules, and the newly formed bone covered the rough surface of the material. The current study did not prove directly the significance of the microporous structure, but this data may support the idea that the microporous modification within each macropore is beneficial for osteoconduction and osteointegration in PLF.

From the distinct histological difference among three HA groups, there may be a fundamental difference between the non-interconnected porous HA and the interconnected porous HA in the role as bone graft extenders in PLF. The non-interconnected porous HA did not integrate with newly formed bone even in fusion mass which obtained solidity. This result indicates that the non-interconnected porous HA works only as a space maintainer and that the newly formed bone around the HA granules plays a role in stabilizing the operative segment. The implanted HA without osteointegration will obstruct bone remodeling in fusion mass, and will result in heterogeneous bone tissue [23]. On the other hand, the interconnected porous HA85% granules obtained an excellent unification with the newly mineralized bone in fusion mass. Despite the existence of the HA granules, the fusion mass consisted of a relatively homogenous trabecular structure. In other words, the HA85% works as a scaffold for newly formed bone, and the trabecular bone both inside and outside the HA granules firmly connect each other to provide structural support in PLF.

On the contrary to the histological results, the porous modification of HA has little influence on fusion rate and mechanical strength in this PLF model. In an environment of metaphyseal bone defect, the interconnected high porous HA could obtain excellent mechanical outcomes in correlation with bone ingrowth within materials as previously reported [29]. However, the histological superiority of BIR and BAR in the HA85% group was not consistent with that of the fusion rate and mechanical strength in this PLF model. This is probably because primary stabilization of the fusion segment may be achieved by bridging bone between the adjacent transverse processes outside the implanted materials, rather than the degree of integration between the newly formed bone and the granules in PLF. This speculation is supported by our result that there was no difference either in BV/TV_{out} and/or fusion rate between the three HA groups, whereas the higher fusion rate in the Auto group will be consistent with the higher BV/TV. We believe that porous modification of HA only is insufficient to promote bone formation outside materials in PLF because HA does not have the ability of osteoinduction.

Despite the superiority of the HA85% in osteoconduction and osteointegration, a high porous material is always accompanied by a problem of fragility as a bone graft substitute. Initial compressive strength of the HA85% is only 2.0 MPa, which is equivalent to cancellous bone, but failure of the granules could not be seen in this PLF model. This is because the environment of a grafted site in PLF is initially non-weight bearing and fusion mass gradually

begins to play a role in load-transmission with its maturation [17]. Therefore, bone graft substitutes in PLF mainly require the capability for bone formation rather than initial mechanical strength. It is supposed that the interconnected high porous HA would be a rational material for a bone graft extender in PLF.

The current study includes some potential design limitations. First, the bone healing capability of rabbits is much higher than that of humans as previously reported [4] and therefore, all the findings of this study might not be applicable to clinical PLF. Benefits of superior osteointegration ability of the HA85% to the non-interconnected porous HAs became obscure by rapid bridging bone formation outside the implant in this rabbit model, however, the findings that the porous modifications of HA had little influence on primary stabilization of the fusion segment is possibly true of clinical PLF. Because bridging bone generated by autogenous bone graft is more easily and rapidly achieved than bone ingrowth to the implanted HA, it seems reasonable to suppose that bridging bone formation through the interval between the HA granules precedes the bone ingrowth to the HA when HA is used as a bone graft extender even in clinical PLF. Second, we carried out the evaluations only at 5 weeks. Because Boden et al. [5, 6] reported that if solid fusion was not seen after 5 weeks, assessment at longer time points did not show an increase in the fusion rate or the biomechanical properties of the fusion mass in this rabbit PLF model. Since the fusion mass in the Auto group obtained solidity at 5 weeks in our results, this time point seemed to allow the adequate evaluation of the mechanical outcomes in this model. However, long-term effects of HA porous characteristics on the histological outcomes must be examined. Finally, we should also pay attention to the influence of HA granule size on healing outcomes especially in the non-interconnected porous HA groups. Because of few interconnecting pores, the fusion mass would gradually become more heterogeneous as the granule size of the non-interconnected porous HA increases.

The current study demonstrated that the HA porous characteristics had an effect on the histological outcomes in a rabbit PLF model. The interconnected high porous structure seems to be promising for the environment of PLF in the point of producing fusion mass with higher cellular viability. This is because the HA85% is superior in terms of integration with the newly formed bone in fusion mass compared to the non-interconnected porous HAs. However, the porous modifications of HA have little influence on fusion rate and mechanical strength because primary stabilization of the fusion segment is mainly achieved by bridging bone between the adjacent transverse processes outside the implanted materials, rather than the degree of integration between the newly formed bone and the HA granules in PLF.

Acknowledgments The authors would like to acknowledge Michiko Sakamoto, B.S., PENTAX Co., for their technical support and for providing materials. They are also grateful to Mr. Justin Collings for correcting their use of language. This study was supported by PENTAX Co.

References

1. Akazawa T, Murata M, Sasaki T (2006) Biodegradation and bioabsorption innovation of the functionally graded bovine bone-originated apatite with blood permeability. J Biomed Mater Res A 76(1):44–51
2. Annaz B, Hing KA, Kayser M (2004) Porosity variation in Hydroxyapatite and Osteoblast morphology: a scanning electron microscopy study. J Microsc 215(Pt 1):100–110
3. Berven S, Tay BK, Kleinstueck FS (2001) Clinical applications of bone graft substitutes in spine surgery: consideration of mineralized and demineralized preparations and growth factor supplementation. Eur Spine J 10(Suppl 2):S169–S177
4. Boden SD (2002) Overview of the biology of Lumbar spine fusion and principles for selecting a bone graft substitute. Spine 27(16 Suppl 1):S26–S31
5. Boden SD, Martin GJ Jr, Morone M (1999) The use of Coralline Hydroxyapatite with bone marrow, autogenous bone graft, or osteoinductive bone protein extract for posterolateral Lumbar spine fusion. Spine 24(4):320–327
6. Boden SD, Schimandle JH, Hutton WC (1995) 1995 Volvo Award in basic sciences. The use of an osteoinductive growth factor for lumbar spinal fusion. Part Ii: Study of dose, carrier, and species. Spine 20(24):2633–2644
7. Boden SD, Schimandle JH, Hutton WC (1995) An experimental lumbar intertransverse process spinal fusion model. Radiographic, histologic, and biomechanical healing characteristics. Spine 20(4):412–420
8. Chang BS, Lee CK, Hong KS (2000) Osteoconduction at porous hydroxyapatite with various pore configurations. Biomaterials 21(12):1291–1298
9. Flautre B, Descamps M, Delecourt C (2001) Porous ha ceramic for bone replacement: role of the pores and interconnections—experimental study in the rabbit. J Mater Sci Mater Med 12(8):679–682
10. Fujishiro T, Nishikawa T, Niikura T (2005) Impaction bone grafting with hydroxyapatite: increased femoral component stability in experiments using sawbones. Acta Orthop 76(4):550–554
11. Glazer PA, Heilmann MR, Lotz JC (1997) Use of electromagnetic fields in a spinal fusion. A rabbit model. Spine 22(20):2351–2356
12. Habibovic P, Yuan H, van der Valk CM (2005) 3D Microenvironment as essential element for osteoinduction by biomaterials. Biomaterials 26(17):3565–3575
13. Hing KA (2004) Bone repair in the twenty-first century: biology, chemistry or engineering? Philos Transact A Math Phys Eng Sci 362(1825):2821–2850
14. Hing KA, Annaz B, Saeed S (2005) Microporosity enhances bioactivity of synthetic bone graft substitutes. J Mater Sci Mater Med 16(5):467–475
15. Hing KA, Best SM, Tanner KE (2004) Mediation of bone ingrowth in porous hydroxyapatite bone graft substitutes. J Biomed Mater Res A 68(1):187–200
16. Ito M, Kotani Y, Hojo N, (2007) Effects of porosity changes in hydroxyapatite ceramics vertebral spacer on its binding capability to the vertebral body: an experimental sheep study. J Neurosurg 6(5):431–437

17. Kanayama M, Cunningham BW, Weis JC (1997) Maturation of the posterolateral spinal fusion and its effect on load-sharing of spinal instrumentation. An in vivo sheep model. J Bone Joint Surg Am 79(11):1710–1720
18. Liu DM (1996) Fabrication and characterization of porous hydroxyapatite granules. Biomaterials 17(20):1955–1957
19. Lu JX, Flautre B, Anselme K (1999) Role of interconnections in porous bioceramics on bone recolonization in vitro and in vivo. J Mater Sci Mater Med 10(2):111–120
20. Luchetti R (2004) Corrective osteotomy of malunited distal radius fractures using carbonated hydroxyapatite as an alternative to autogenous bone grafting. J Hand Surg 29(5):825–834
21. Matsumine A, Myoui A, Kusuzaki K (2004) Calcium hydroxyapatite ceramic implants in bone tumour surgery. A long-term follow-up study. J Bone Joint Surg Br 86(5):719–725
22. Moritz N, Rossi S, Vedel E (2004) Implants coated with bioactive glass by Co_2-Laser, an in vivo study. J Mater Sci Mater Med 15(7):795–802
23. Orr TE, Villars PA, Mitchell SL (2001) Compressive properties of cancellous bone defects in a rabbit model treated with particles of natural bone mineral and synthetic hydroxyapatite. Biomaterials 22(14):1953–1959
24. Rosa AL, Beloti MM, Oliveira PT (2002) Osseointegration and osseoconductivity of hydroxyapatite of different microporosities. J Mater Sci Mater Med 13(11):1071–1075
25. Rouahi M, Gallet O, Champion E (2006) Influence of hydroxyapatite microstructure on human bone cell response. J Biomed Mater Res A
26. Sakamoto M, Matrumoto T, Nakasu M (2007) Development of super porous hydroxyapatites and their utilization for culture of primary rat osteoblast. J Biomed Mater Res A 82(1):238–242
27. Spivak JM, Hasharoni A (2001) Use of hydroxyapatite in spine surgery. Eur Spine J 10(Suppl 2):S197–S204
28. Summers BN, Eisenstein SM (1989) Donor site pain from the ilium. A complication of lumbar spine fusion. J Bone Joint Surg Br 71(4):677–680
29. Tamai N, Myoui A, Tomita T (2002) Novel hydroxyapatite ceramics with an interconnective porous structure exhibit superior osteoconduction in vivo. J Biomed Mater Res 59(1):110–117
30. Totoribe K, Tajima N, Chosa E (2002) Hydroxyapatite block for use in posterolateral lumbar fusion: a report of four cases. Clin Orthop Relat Res 399:146–151
31. Wiltse LL, Bateman JG, Hutchinson RH (1968) The paraspinal sacrospinalis-splitting approach to the lumbar spine. J Bone Joint Surg Am 50(5):919–926
32. Ylinen P, Raekallio M, Taurio R (2005) Coralline hydroxyapatite reinforced with polylactide fibres in lumbar interbody implantation. J Mater Sci Mater Med 16(4):325–331
33. Younger EM, Chapman MW (1989) Morbidity at bone graft donor sites. J Orthop Trauma 3(3):192–195
34. Yuan H, Kurashina K, de Bruijn JD (1999) A preliminary study on osteoinduction of two kinds of calcium phosphate ceramics. Biomaterials 20(19):1799–1806